Jamming percolation and glassy dynamics

Cristina Toninelli[*]and Giulio Biroli[†]

Abstract

We present a detailed physical analysis of the dynamical glass-jamming transition which occurs for the so called Knight models recently introduced and analyzed in a joint work with D.S.Fisher [15]. Furthermore, we review some of our previous works on Kinetically Constrained Models.

The Knights models correspond to a new class of kinetically constrained models which provide the first example of finite dimensional models with an *ideal glass-jamming transition*. This is due to the underlying percolation transition of particles which are mutually blocked by the constraints. This *jamming percolation* has unconventional features: it is discontinuous (i.e. the percolating cluster is compact at the transition) and the typical size of the clusters diverges faster than any power law when $\rho \nearrow \rho_c$. These properties give rise for Knight models to an ergodicity breaking transition at ρ_c: at and above ρ_c a finite fraction of the system is frozen. In turn, this finite jump in the density of frozen sites leads to a two step relaxation for dynamic correlations in the unjammed phase, analogous to that of glass forming liquids. Also, due to the faster than power law divergence of the dynamical correlation length, relaxation times diverge in a way similar to the Vogel-Fulcher law.

Keywords: Kinetically constrained lattice gases, glassy dynamics, bootstrap percolation, jamming transition.

[*]Institut des Hautes Études Scientifiques, Le Bois-Marie 35, Route de Chartres F-91440 Bures-sur-Yvette, FRANCE

[†]Service de Physique Théorique, CEA/Saclay-Orme des Merisiers, F-91191 Gif-sur-Yvette Cedex, FRANCE

1 Introduction

The formation of amorphous solids as glasses and granular media, i.e the *glass and jamming transitions*, are still unsettled and fascinating questions in condensed matter physics despite all the works that have been devoted to this subject. These phenomena occur in a variety of systems which, even if microscopically very different, share common features. Among the others we recall supercooled liquids, colloidal suspensions and non-thermal jamming systems (e.g. vibrated granular materials) [1–3]. Basic *glassy properties* include a dramatic slowing down of dynamics when a proper external parameter is tuned (e.g. temperature is lowered for liquids) and the occurrence of a complicated relaxation: non exponential and spatially heterogeneous [4]. When relaxation times become longer than experimental scales, equilibrium can no more be achieved and the systems freeze into an amorphous phase.

Even the basic issues in understanding these phenomena remain unsolved. In particular, it is not settled whether the dynamical arrest is due to the proximity of a phase transition and whether this putative phase transition is a static or purely dynamical one. However experiments make it clear that, if an *ideal glass transition* occurs, it should have an unconventional behavior with mixed first and second order features. On the one hand, the divergence of relaxation times and the fact that both entropy and internal energy seem continuous (for molecular liquids) is indicative of a second order transition. On the other hand, there is a discontinuous order parameter: the infinite time limit of the Fourier transform of the density–density correlation (analogous to Edwards-Anderson parameter for spin glasses) has a finite jump at the transition. This corresponds to the fact that the modulation of the microscopic density profile of the glass does not appear continuously from the flat liquid profile (we generally refer for all systems to glass and liquid phase meaning the regime before and after the freezing into an amorphous solid). Besides these mixed first/second order properties, another unconventional feature, compared to usual phase transitions, concerns the scaling of relaxation times. Different functional forms have been proposed in the literature. A very popular and successful representation is the Vogel-Fulcher law. This suggests that the *logarithm* of the relaxation time diverges as the inverse of the distance from the transition, i.e. $\log \tau \simeq 1/T - T_0$, for molecular liquids. Finally, one of the most puzzling features is the absence of any experimental evidence of a static diverging correlation length. In particular, the dramatic slowing down of dynamics does not seem to be due to an increasing long

range order as for e.g. ferromagnetic transition: typical glass configurations are not very different from instantaneous configurations of the liquid. An enormous amount of theoretical approaches have been proposed in the last fifty years to describe these physical phenomena. However, if one takes the *a priori assumption* that a real glass or jamming phase transition takes place at a finite temperature T_c (at a density less than the close-packed one for the jamming transition) then the number of scenarii reduces drastically. Leaving aside very phenomenological ones, there remain only two: either a very subtle static transition occurs (random first order scenario [5]) or the transition is purely dynamical. The first possibility invokes [5] a thermodynamic transition similar to the one occurring for the so called discontinuous spin glass models, e.g. REM and p-spin models [6]. This is a one step replica symmetry breaking transition with a discontinuous (Edwards-Anderson) order parameter but no discontinuity for energy and entropy. This approach has been successful in explaining and predicting many physical phenomena related to the glass transition [7]. Although mean field models upon which it is based are very well understood by now, some of the finite dimensional predictions are still semi-phenomenological and need further theoretical works to be put on a firm and solid basis, see [8–11] for recent works in this direction. The possibility of a purely dynamical glass transition have been mainly investigated through the so called Kinetically Constrained Models (KCM) ([12]— [41] and references therein). These are stochastic lattice gases based on the ansatz that glass or jamming transitions are due to effective geometrical constraints on the rearrangements of the atoms or molecules generated close to the transition. Static correlations beyond those present in dense liquids are assumed to play no role. Recently, in a joint work with D.S.Fisher [15], we have shown that indeed some KCMs display a purely dynamical transition on finite dimensional lattices with the basic features of the previously described glass-jamming transition.

Note that these two scenarii are not necessarily in contrast because it might well be that, despite similar behaviors, the glass-jamming transition in molecular liquids, colloids and granular media are of different origin. The thermodynamic scenario might apply to the glass transition of molecular liquids whereas jamming transitions might correspond to purely dynamic phase transitions.

Here we give an extended explanation of the result in [15] and we review some of our previous works (and some others when needed) on KCM. We focus in particular on the different behaviors and tools needed to deal with

different choices of the stochastic dynamics. This paper is not intended to be an extensive review on KCMs: for all the results previous to our works we refer to the reviews [12, 13] and references therein, while some more recent results for kinetically constrained spin models can be found in [20–23].

The outline of the paper is the following. In Section 2 we introduce the models distinguishing those with Glauber (KCSM) and Kawasaki (KCLG) dynamics and further dividing both classes into cooperative and non cooperative models. In Section 3 we review the different types of dynamical arrest that occur and motivate the analysis of KCMs from a theoretical point of view. In Section 4 we present tools and results for non cooperative models. In Section 5 we describe the jamming transition that cooperative KCMs display on Bethe lattices. In Section 6 we discuss the class of cooperative models (Knight models) introduced in [15, 37] proving that they display an ideal glass transition. In particular, we show that this transition is related to a new type of percolation transition, which we call *jamming percolation*. In this Section we also explain which are the tools one needs in general to study cooperative KCMs, using Knight models as an example. Finally, we present our conclusions in Section 7.

2   Kinetically Constrained Models (KCM)

KCMs are stochastic lattice gases with hard core exclusion, that is on each site there can be one or zero particle. In other words, a configuration on a lattice Λ is given by the set of two-valued occupation variables on each site $x \in \Lambda$: $\eta_x = \{1, 0\}$. These represent occupied and empty sites (particles and vacancies), respectively. The dynamics is given by a continuous time Markov process which consists of a sequence of jumps for models with conservative (Kawasaki) dynamics and birth/death for models with non conservative (Glauber) dynamics. The former are also known as Kinetically Constrained Lattice Gases (KCLG), the latter as Kinetically Constrained Spin Models (KCSM) or facilitated spin models ($\eta_x = \{1, 0\}$ are interpreted as spin up and spin down). For all the models we consider, dynamics satisfies detailed balance w.r.t. Bernoulli product measure, μ_ρ, at density ρ. Thus, there are no static interactions beyond hard core and an equilibrium transition cannot occur. However, in order for a move to be allowed, it is not enough to verify the hard core constraint. Indeed the jump or birth/death rates are non zero only if the configuration satisfies some additional local constraints, hence the

4

name *kinetically constrained*. These mimic the geometric constraints on the possible rearrangements in physical systems, which could be at the root of the dynamical arrest [14, 17]. For example, in a highly dense liquid, numerical simulations [38] have shown that a molecule is caged by its neighbors and it cannot move on a substantial distance unless the neighbors move and the "cage is opened". Experimental evidence of such *cage effect* for colloidal suspensions and granular materials have indeed been detected [3, 39].

Numerical simulations show that, for proper choices of the constraints, KCM display glassy features including stretched exponential relaxation, super-Arrhenius slowing down and dynamical heterogeneities [13]. Therefore, despite their simplified and discrete character they could capture the key ingredients of glassy dynamics, at least on proper time scales. Indeed, several works have been recently devoted to understanding the mechanism which induces these glassy properties and evaluating the typical time/length scales involved.

2.1 Kinetically Constrained Spin Models (KCSM)

KCSMs are endowed with a non conservative dynamics: each site changes from occupied to empty and from empty to occupied with rate $(1 - \rho)f_x(\eta)$ and $\rho f_x(\eta)$, respectively. The value of $f_x(\eta)$, which encodes the kinetic constraints, does not depend on η_x. Thus detailed balance is satisfied with Bernoulli product measure, μ_ρ, at density ρ.

KCSMs can be divided into two classes : non-cooperative and cooperative ones. For the former it is (for the latter it is not) possible to construct an allowed path which completely empties *any* configuration provided a proper finite cluster of vacancies is present somewhere. We call this cluster a *defect*. Among non cooperative models we recall the Fredrickson-Andersen [14] one spin facilitated (FA1f). For FA1f a move in x is allowed only if at least one of the nearest neighbors is empty: $f_x(\eta) = 1$ if $\sum_{y \; n.n.x}(1 - \eta_x) > 0$, $f_x(\eta) = 0$ otherwise. This has recently received a renewed attention, especially since it has been proposed as a model for strong glasses [25]. It is easy to check that the presence of a single vacancy in this model allows one to empty the whole lattice.

Among cooperative models we recall FAf on an hyper-cubic lattice of dimension d with $2 \le f \le d$ [14]. Here the constraint requires that at least f of the surrounding sites are empty in order for the birth/death rate to be non zero. As can be directly checked, for all these models it is not possible to devise

a finite seed of vacancies which allows emptying the whole lattice. Consider, e.g., the case $d = 2$, $f = 2$ (with periodic boundary conditions) and focus on a configuration which contains two adjacent rows which are completely filled. These particles can never be erased, even if the rest of the lattice is completely empty: it does not exist a finite defect which can destroy them, thus the model is cooperative. The restriction on f comes from the fact that all cases $f > d$ are very special because at any value of ρ there exist finite sets of forever blocked particles, namely a fraction of the system is frozen at all densities. Although they might be interesting in themselves, they do not seem suitable to describe the slow dynamics close to glass-jamming transition because they are non-ergodic at any temperature/density.

A different class of cooperative models is the one we introduced in [15], which we call Knight models. On a square lattice kinetic constraints are the followings: a move on x can occur only if [the two North-East *or* the two South-West fourth nearest neighbors are empty] *and* [the two North-West *or* the two South-East forth nearest neighbors are empty]. The definition of the North-East, South-East, North-West and South-West neighbors and an example of the constraints is given in Fig.1. In formulas $f_x(\eta) = f_x(\eta)^{NE-SW} f_x(\eta)^{NW-SE}$ where

$$f_x(\eta)^{NE-SW} = [(1 - \eta_{NE1_x})(1 - \eta_{NE2_x}) + (1 - \eta_{SW1_x})(1 - \eta_{SW2_x})]$$

$$f_x(\eta)^{NW-SE} = [(1 - \eta_{SE1_x})(1 - \eta_{SE2_x}) + (1 - \eta_{NW1_x})(1 - \eta_{NW2_x})]$$

with $NE1_x = x + 2e_1 + e_2$, $NE2_x = x + e_1 + 2e_2$, $SW1_x = x - 2e_1 - e_2$, $SW2_x = x - e_1 - 2e_2$, $SE1_x = x + 2e_1 - e_2$, $SE2_x = x + e_1 - 2e_2$, $NW1_x = x - 2e_1 + e_2$ and $NW2_x = x - e_1 + 2e_2$.

Finally, we recall the one-dimensional East model. In this case the constraint requires a vacancy on the right nearest neighbors, that is $f_x = (1 - \eta_{x+1})$. Note that on a finite lattice the presence of a single vacancy on the rightmost site allows to empty the whole lattice. However the model does not belong to the above defined non-cooperative class, since the vacancy should occur in a specific position. Indeed, it is usually classified as cooperative: due to the direct nature of constraints the relaxation involves the cooperative rearrangements of large regions as $\rho \nearrow 1$ [18–20].

2.2   Kinetically Constrained Lattice Gases (KCLG)

KCLG are endowed with a conservative dynamics. A particle in x attempts at a fixed rate to jump to a random nearby empty site y and the move
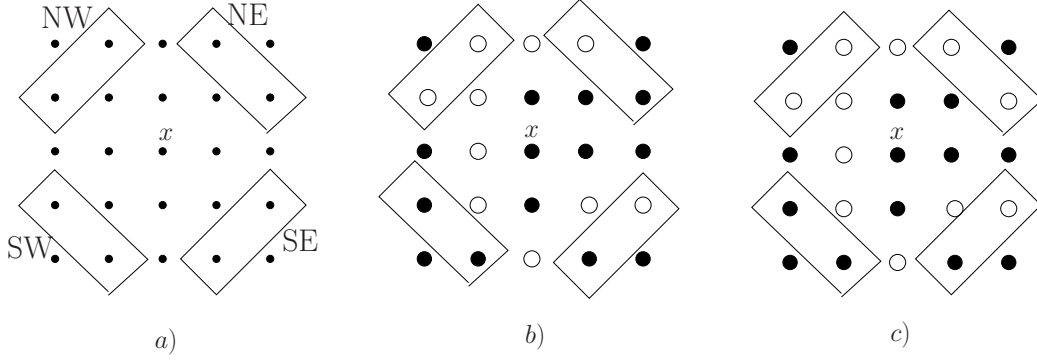
Figure 1: a) Site x and the four couples of its North-East (NE), South-East (SE),North-West (NW), South-West (SW)neighbours. b) Filled (empty) circles stand for filled (empty) sites. Here x is occupied and cannot be emptied because in the NorthEast-SouthWest direction none of the two couples is completely empty. c) Same configuration as in b) except for site $x + 2\,e_1 + e_2$ which is empty. Here x can be emptied since both its NW and both its NW neighbours are empty, which guarantees $\eta \in \mathcal{A}_x$.

occurs with rate $\eta_x(1 - \eta_y)f_{x,y}(\eta)$. Here $f_{x,y}(\eta)$ does not depend on the configuration on x and y. Since dynamics preserves the number of particles, detailed balance on finite volume is satisfied w.r.t. the measure which is uniform on configurations with fixed particle number. On the other hand, on infinite volume detailed balance holds w.r.t any Bernoulli product measure μ_ρ. Again, we can classify KCLG as non-cooperative and cooperative models. For the former it is (for the latter it is not) possible to construct a finite group of vacancies such that for *any* configuration it can be moved all over the lattice and any jump of a particle to a neighboring empty site can be performed when the particle is adjacent to the empty cluster. We will call this mobile cluster which facilitates jumps a *macrovacancy*. As can be immediately checked the model in which there are no further kinetic constraints besides hard core, the so called normal lattice gas or symmetric simple exclusion process (SSEP), is non cooperative and the minimal macrovacancies are simple vacancies.

Among cooperative models we recall Kob Andersen model (KA) [17] on a cubic lattice. Here a particle can jump to a neighboring site only if both in the initial and final position at least m of its nearest neighbors are empty, where $m = 3$. Analogously, one can define KA models on hyper-cubic lattices

7

of dimension d and for different values of the parameter m, with $2 \leq m \leq d$. The restrictions on m are due to the fact that $m = 1$ corresponds to SSEP while a model with $m > d$ has a finite fraction of particles that is frozen at any density (cf. FA models with $f \geq d + 1$). Again, one can directly check that all these models are cooperatives according to the definition above. Consider, e.g. KA in $d = 3$ with $m = 3$ and focus on a configuration containing a completely filled slab which spans the lattice and has a two by two transverse section. Any finite cluster of vacancies can never overcome this filled structure, therefore it is not possible to construct a finite macrovacancy that moves everywhere in the lattice. Another possible choice of cooperative KCLG are conservative Knight models [15] defined as follows. A move from x to y occurs only if the configuration satisfies the requirement needed to allow the move in x *and* in y for the non conservative Knight model defined in previous section (plus y should be empty).

On the other hand, an example of a non cooperative KCLG is provided by KA model with $m = 2$ on a triangular lattice. Indeed, two neighboring vacancies form the required mobile macrovacancy as will be further explained in Section 4.

3   Glass-jamming transition in KCM

3.1   Ergodicity breaking and glass-jamming transitions

Let us take the point of view that glass and jamming transitions observed in experiments are not just cross-overs but they do correspond to a real thermodynamic or dynamic phase transition. For simplicity we will focus on lattice models assuming that the presence of the underlying lattice does not change qualitatively the physics.

As explained in the Introduction, from the experiments it is clear that *ideal glass-jamming transitions* (if they exist) have peculiar features compared to standard first or second order phase transitions. In particular, they are characterized by a diverging timescale although no growing static correlation lengthscale has ever been found, contrary to second order phase transition where the relaxation timescale diverges because long-range thermodynamic order sets in. This strongly suggests that ideal glass-jamming transitions are purely dynamic phase transitions, i.e. they are characterized by an ergodicity breaking without any singularity in the thermodynamics.

Is it possible? This question has been addressed in the mathematical physical literature (see [42] for a detailed discussion) focusing on interacting hard core particle systems on finite dimensional lattices. If particles interact via a short-range potential and the rates for exchanging a particle with a nearest neighbor vacancy are always strictly positive then it has been proved that in two dimensions the ensemble of the Gibbs measures, $\mathcal{G}$, coincides with the ensemble of stationary (under the dynamical evolution) measures. In higher dimensions it has been proved that $\mathcal{G}$ coincides with all reversible stationary measures, where reversible measure means (roughly speaking) that it verifies detailed balance. It is not known if there exist stationary non reversible measures. It seems unlikely because they would lead to circulating probability currents without any net injection of energy inside the systems, see [42]. In any case they are certainly not relevant for the problem of the glass transition. Thus, as far as glass-jamming transitions are concerned, one can safely assume (as it has been proved in two dimensions) that the ensemble of Gibbs measures coincides with the ensemble of stationary measures. Therefore, if a dynamical transition takes place, this would lead to more than one stationary measure and as a consequence to more than one Gibbs measure: dynamical transitions has to be accompanied by thermodynamic transition.

Would this mean that the ideal glass-jamming transitions must be only of thermodynamic origin and no pure dynamical transition can take place? This is puzzling, because the absence of any indication of growing static correlation lengths seems to be at odds with the very existence of a thermodynamic transition inducing a diverging relaxation time. If one does not want to let down the assumption that experimental glass-jamming transitions correspond to real phase transitions there remains mainly two possibilities. A thermodynamic transition indeed takes place but it is of a completely new type and such that is not visible in any given $n-$point correlation function. A good candidate for that is the Random First Order Theory [7]. Otherwise, some hypothesis that lead to the previous conclusion (no purely dynamical transition) must be violated. The only one that is reasonable to violate on physical grounds is the fact that the rates for exchanging a particle with a nearest neighbor vacancy have to be strictly positive. Consider for example hard spheres with Brownian or Monte Carlo dynamics (that is a reasonably good model for colloidal or even granular systems displaying glass-jamming transitions). If the density is high enough some moves can have rate zero. This can have a dramatic consequence on the dynamics because now the configuration space can be broken into subsets that are not connected by any
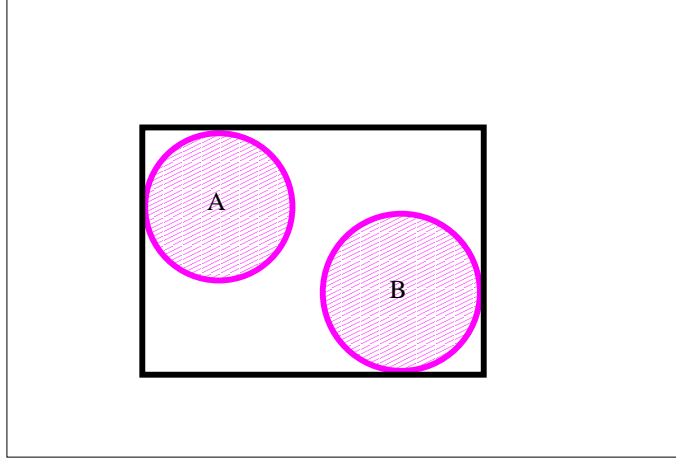
9

Figure 2: The configuration space of the two discs in the box is broken in disconnected components. It is not possible to reach dynamically the configuration with the disk A in the position of B and viceversa.

dynamical move when density is large enough, see Fig.2 for a trivial example. Formally, the Markov chain associated to the dynamical evolution becomes reducible contrary to the case of the lattice gas with strictly positive rates.

As a conclusion the only possibility of having a purely dynamic transition seems to boil down to having zero (i.e. degenerate) rates depending on the configuration around a site. This encodes the physical effect explained previously, see also Fig. 2, that is certainly present for systems of hard objects as colloids and granular media. The dynamical transition that may be induced by degenerate rates is a reducible-irreducible phase transition. At low density (high temperature) almost any equilibrium configuration is contained in the same ergodic component. Instead, at high density (low temperature), the configuration space sampled with the equilibrium measure is fractured in many different components (and no one of them covers almost all the space). KCMs are the simplest model that take this phenomenon into account. Because of their simplicity they allow to study in great detail the issue of glass-jamming transition as purely dynamical transition.

Indeed for KCMs (see Section 2) some rates are zero, hence their name *kinetically constrained*, and this implies that the configuration space on fi-

nite lattices is generically reducible. In particular, there exist configurations which cannot be connected one to the other using allowed moves. For example, for FA model with $f = 2$ and $d = 2$ (see Section 2.1), a configuration which is empty with the exception of two adjacent rows which are completely filled can never be connected to any configuration which does not contain this slab. This implies that on any finite volume Λ the process is not ergodic and μ_ρs are not the unique invariant measures. The crucial issue is whether ergodicity is restored in the thermodynamic limit and whether this depends upon the value of ρ.

Two final remarks are in order. First, as shown in [36, 40], thanks to the product form of the equilibrium measure, for KCMs establishing ergodicity at density ρ corresponds to proving that there exists an irreducible set of configurations[1] (i.e. configurations connected one to the others by allowed paths) which has unit probability w.r.t. μ_ρ in the thermodynamic limit. Another way to put it is that the only possible way of breaking ergodicity is by the reducible-irreducible transition discussed above. The second remark is that this type of transition is very different from the critical slowing down related to second order phase transitions. In those cases the ergodicity breaking is induced by the thermodynamic limit (the number of degrees of freedom goes to infinity and so the relaxation time may go to infinity). Instead, for the type of dynamical transition advocated above, finite size systems are typically non ergodic and the crucial question is whether in the thermodynamic limit the ergodicity is restored and up to which density.

3.2 Dynamical transition in KCMs and jamming-bootstrap- $k$core percolation

For non-cooperative models it is immediate to conclude that ergodicity holds at any density $\rho < 1$. Indeed, the probability of finding at least a defect or a macrovacancy for an equilibrium configuration goes to one in infinite volume. Starting from this macrovacancy, by definition of non-cooperative KCSM, one can empty all the lattice. Therefore, two typical equilibrium configurations are almost surely connected by a path (with strictly positive rates) in the configuration space. The situation is similar for non-cooperative

---

[1]More precisely, we should identify a sequence of sets $\mathcal{F}_L$ on $0, 1^{|\Lambda_L|}$ such that $\mathcal{F}_L$ is irreducible w.r.t. the chosen dynamics on Λ_L with periodic boundary conditions and $\lim_{L\to\infty} \mu_\rho(\mathcal{F}_L) = 1$.

KCLG. In this case configurations with a macrovacancy can be connected by a path which subsequently performs all nearby particle exchanges by previously moving the macrovacancy near the interested sites.

The case of cooperative KCMs is much more involved and indeed it can lead to an ergodicity breaking transition. In general, as discussed previously, in order to prove ergodicity one should construct an irreducible set and prove that it has unit probability w.r.t. μ_ρ in the thermodynamic limit. For KCSMs (with periodic boundary conditions) the relevant irreducible set is composed by configurations that can be completely emptied by allowed moves, as it can be found easily analyzing these systems at low density. This component can be identified by the following deterministic procedure: subsequently remove all particles for which the constraint is verified until reaching a completely empty configuration or one in which there is a backbone of mutually blocked particles. Note that this backbone is uniquely determined by the initial configuration: it does not depend on the chosen order to erase particles. If the backbone is empty, we say that the configuration is *internally spanned* and, by definition, it belongs to the relevant irreducible component. Therefore, ergodicity breaking takes place if and only if equilibrium configurations contain an infinite backbone of blocked sites in the thermodynamic limit. Note that,as discussed previously, we will consider only choices of the constraints such that a blocked cluster has necessarily to be infinite.

Thus, the problem of the existence of an ergodicity breaking transition for cooperative KCSMs can be reformulated as a percolation transition for the final configuration of the above cellular automata. For FA models the latter coincides with bootstrap percolation procedure [43,44] or k-core percolation [45]: a particle is removed if it has less than m neighbors. The results in [44, 46] establish that bootstrap percolation converges to a completely empty lattice for all $\rho < 1$, namely no percolation transition occurs. Therefore, it is immediate to conclude that FAf on any hyper-cubic d-dimensional lattice does not display an ergodicity breaking transition at any $\rho < 1$ for all f and d. On the contrary, for the cellular automata corresponding to Knight models, a *jamming percolation* transition (as we called it) occurs at a critical density $\rho_c < 1$ as proved in [15, 37]. Therefore, Knight models in infinite volume are ergodic for $\rho < \rho_c$ and non ergodic for $\rho \geq \rho_c$. In Section 6 we will explain the mechanism which induces the percolation transition for the blocked structures of Knight models and discuss its character.

For cooperative KCLG, the prove of ergodicity is more involved. For example, for KA model on square lattices with $m = 2$, we have shown that the

irreducible component which has unit probability in the thermodynamic limit is the one composed by configurations which can be connected by an allowed path to a configuration which have a frame of vacancies on the boundary [36]. Establishing that this set has unit probability in the thermodynamic limit is more involved than in the corresponding KCSM (i.e. FA model). This is due to the fact that there do not exist a deterministic bootstrap-like procedure which allows to establish whether a configuration belongs or not to the irreducible set.

Finally note that, apart from ergodicity breaking, other types of transition might take place in lattice models for glass-jamming transitions: (1) a change from an exponential to a *stretched exponential relaxation* for density-density correlation in KCSM or its Fourier transform for KCLG, (2) a *diffusive/subdiffusive transition* in the behavior of a probe particle and (3) a *break down of the conventional hydrodynamic limit*.

In the case of cooperative KCSM numerical simulations [17, 29–31] seems to indicate that connected correlation functions, e.g. $< \eta_x(t)\eta_x(0) >_\rho - < \eta_x(t) >_\rho< \eta_x(0) >_\rho$, decay in time as stretched exponential, $\exp[-(t/\tau)^\beta]$, with a stretched exponent β that is less than one and density dependent (β decreases as ρ is increased). Analytical works based on mode coupling approximations [28] support these results. The standard explanation of this behavior is dynamic heterogeneity, which has indeed been experimentally detected [4] and consists in having different relaxation times in different regions of the system. The superposition of these exponential relaxations would then lead to an *effective* stretched exponential behavior.

Although this is likely what happens for KCSMs and real liquids, it has been recently proved in [23] that relaxation is exponential at very large times for all cooperative and non-cooperative models (in the ergodic regime) considered so far. More precisely, relaxation is exponential on times of the order of the inverse of the spectral gap of the Liouvillian operator generating the dynamics (that is the slowest relaxation time over all one time quantities) and this is proved to be finite at any ρ in the ergodic regime. The discrepancy between rigorous and numerical results is likely due to the different time regimes that are investigated: a correlation function can be well approximated as a stretched exponential for times t of the order of its relaxation time [2] τ and decay as an exponential when $t >> \tau$. An interesting question

---

[2]Here we mean the time over which the specific normalized connected correlation function has decayed to e^{-1}, which may of course be shorter than the slowest relaxation time

13

is whether the effective numerical behavior coming from fit on times of the order of τ can be made precise: in the scaling limit $\tau \to \infty$, with t/τ of the order of one, do correlation functions converge to stretched exponentials?.

Another transition different from the ergodicity breaking is a diffusive/subdiffusive transition for the motion of tagged particles. The result that the self-diffusion coefficient, $D_s(\rho)$, is positive at any density less than one, which is known to hold for SSEP cannot be immediately extended to KCLG due to the degeneracy of jump rates. In particular for KA models, from numerical simulations [17] it had been conjectured that $D_s > 0$ only below a finite critical density. However, in [40] it has been proved $D_s > 0$ at any density $\rho < 1$ for non-cooperative models and the result have been extended to cooperative models (in the ergodic regime) in [41].

Finally, a third possibility is a breakdown of the conventional hydrodynamic limit that usually holds on long length and time scales [42]. For KCLG, if the constraint is released, the macroscopic density profile evolves via the diffusion equation $\partial_t \rho = \nabla(D(\rho)\nabla\rho)$ where $D(\rho) = 1$ for the normal lattice gas. Again, due to the presence of constraints, one cannot apply the techniques which have been developed to establish this hydrodynamic limit for stochastic lattice gases [47]. Furthermore, for some cooperative KCLG, it has been conjectured [50] that the macroscopic diffusion coefficient $D(\rho)$ would vanish at high density, leading to a sub-diffusive evolution of density profiles. In [48] it is proved that for a class of non cooperative models hydrodynamic limit holds with $D(\rho)$ vanishing (as power law of $1 - \rho$) only for $\rho \to 1$. Extending these results to cooperative models would require establishing the scaling of relaxation times on finite lattices with the size of the lattice, which has not yet been settled for cooperative KCLG.

4 Non-cooperative models as renormalized lattice gases

In Section 3 we explained that, thanks to the presence of the macrovacancies (for KCLG) and defects (for KCSM), in the thermodynamic limit non cooperative models are ergodic at any $\rho < 1$ as it occurs for the corresponding models without kinetic constraints. In this Section we shall explain that the slow dynamics for non cooperative models can be understood in terms
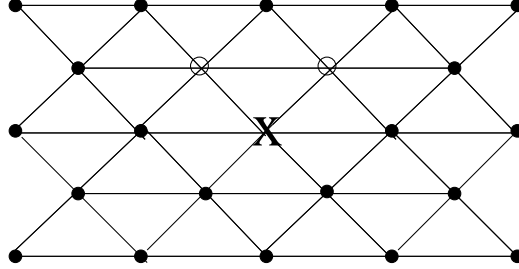
given by the inverse of the spectral gap.

Figure 3: The triangular lattice. For KA with $m = 2$ a particle in x can be moved to the neighbouring empty site $x + (e_1 + e_2)/2$ thanks to the fact that the other empty site $(x + (-e_1 + e_2)/2)$ is nearest neighbors of the particle both in its initial and final position.

of motion of macrovacancies or defects, i.e. as renormalized lattice gases. Indeed these mobile regions, when $\rho \to 1$, essentially perform independent random walks and substantial relaxation takes place only when they pass by. So the high density dynamical behavior is encoded in their properties (size, density, timescale for motion, ...). The analysis and the physical scenario is very similar for non-cooperative KCSM and KCLG. In the following we shall focus on KCLG which are in a sense richer because, apart from the relation timescale, one can study directly the self-diffusion coefficient of tagged particles, D_s, bulk diffusion coefficients, $D(\rho)$, etc.

Let us first focus on the scaling with density of D_s. Consider for example KA model with $m = 2$ on a triangular lattice (see Section 2). The triangular lattice Λ, represented in Fig. 3, is the union of sites in a square lattice Λ_1 and in its dual Λ_2 which is obtained by displacing Λ_1 of $(e_1 + e_2)/2$ with $e_1 = (1, 0)$, $e_2 = (0, 1)$. Two sites $\{x, y\} \in \Lambda$ are nearest neighbors if $x - y = \pm e_1$ or $x - y = \pm(e_1 + e_2)/2$ or $x - y = \pm(-e_1 + e_2)/2$. Dynamics can be reformulated in terms of vacancy motion: a vacancy can move to a neighboring occupied site only if it has at least one empty neighbor both in its initial and final position. Since two neighboring sites of the triangular lattice share a common third neighbor, it is immediate to see that any of the two vacancies of a neighboring couple can move to the common third neighbor. Therefore a couple of neighboring vacancies is a finite size freely mobile cluster. Furthermore it is possible to move any given particle into an empty nearest neighbor provided the couple of vacancies is nearby. For example, if we want to move a particle from x to $x + (e_1 + e_2)/2$ it is sufficient

15

to put the macrovacancy in $x+(e_1+e_2)/2$, $x+(-e_1+e_2)/2$, as shown in Fig.3. Thus, a couple of neighboring vacancies is a macrovacancy according to the definition in Section 2. A simple heuristic argument based on the independent motion of these macrovacancies leads to the correct high density dependence of D_s. Let us focus on dimensions larger than two (for lower dimension the reasoning changes due to recurrent properties of random walks). Call ρ_d the density of macrovacancies and τ_d the timescale on which they move. The self-diffusion coefficient is expected to be proportional to the inverse of the time τ_p on which each particle moves of one step. On the timescale τ_d the number of particles that have jumped is of the order $V\rho_d$ where V is the total number of sites. Thus we find

$$\frac{\tau_p}{\tau_d}V\rho_d \propto V\rho. \tag{1}$$

As a consequence, at density close to one, we get $D_S \propto \rho_d/\tau_d$. Since for the $m = 2$ KA on a triangular lattice macrovacancies are formed by two neighboring vacancies, in the limit $\rho \to 1$ we get $\rho_d \propto (1-\rho)^2$ and $\tau_d \propto O(1)$. Hence, $D_S \propto (1-\rho)^2$. The same arguments leads to $D_S \propto (1-\rho)$ for SSEP, where macrovacancies are single vacancies. The result for SSEP has been rigorously proved in [49] by establishing upper and lower bounds. For KA model on a triangular lattice, as we have shown in [41] (see also [40] for a different choice of non cooperative constraints), it is also possible to turn the heuristic argument into a proof deriving upper and lower bounds $c_l(1-\rho)^2 \leq D_s(\rho) \leq c_u(1-\rho)^2$ with c_u and c_l independent from ρ.

The representation of non-cooperative KCM as renormalized lattice gases turns out to be useful also to obtain these rigorous results. Let us recall the basic strategy since it allows to further understand the role of macrovacancies. The idea is to start from the proof for SSEP in [49] and to modify it by letting macrovacancies play the role of vacancies. The procedure is the following: first construct a suitable auxiliary model that is easy to analyze and then, using a variational formula for D_s, show that $D_s > h(\rho)D_s^{aux}$ where $h(\rho)$ is a function determined explicitly (that is strictly positive for $\rho < 1$). The technique for the upper bound is more classical [49] and the lower bound is more important because it shows that, despite the dynamics slows down, particles still diffuse on large distances and timescales. Therefore, we will just focus on the lower bound in the following.

In [49] the auxiliary model is constructed in this way: the tracer has a neighboring vacancy at time zero and the only possible moves are jumps of

the tracer and exchanges of the occupation variables in y and w, where both y and w are nearest neighbors of the tracer. Note that the latter moves are not allowed for SSEP but one can reconstruct them trough a path of allowed moves thanks to the presence of the vacancy. For the auxiliary model it is immediate to prove that $D_s^{aux} > 0$ and is bounded from above and below by density independent constants. Indeed, a move of the tracer from x to $x + e_i$ can always occur via two steps: since the tracer has always at least one neighboring vacancy, this can be brought (in one move) in $x + e_1$ and then the jump of the tracer from x to $x + e_1$ can occur. Using a variational formula for D_s [49] and comparing the dynamics of the normal lattice gas and the auxiliary model leads to $D_s^{SSEP} > c\,(1 - \rho)\,D_s^{aux}$. The term $(1 - \rho)$ comes from the requirement of having at least a vacancy at time zero near the tracer; c is a density independent constant which accounts for the maximal length of the path needed to exchange the occupation variable in x and w trough neighboring jumps (the only moves allowed for SSEP). For KA on the triangular lattice one defines the following auxiliary process. We require a macrovancancy near the tracer in the initial configuration and we allow only moves which either displace the tracer to a nearest neighbor or move the macrovacancy into another couple of sites which are also near the tracer (for a precise definition of the auxiliary model see [41]). Again, the latter move is not allowed in KA but can be reconstructed by a finite path of allowed moves. As before, it is easy to show that $D_s^{aux} > 0$ and is independent from ρ. Comparing KA and auxiliary dynamics we get $D_s > c\,(1 - \rho)^2$, where $(1-\rho)^2$ comes from the requirement of having a macrovacancy. Note that this procedure is generalizable to all non cooperative models: if the macrovacancy is formed by q empty sites it leads to $D_s(\rho) \geq c(1 - \rho)^q$. Therefore, at least for the motion of the tracer, non cooperative KCLG are simply renormalized SSEP: the typical diffusion time of the tagged particle (i.e. the inverse of D_s) goes here as the inverse of the density of macrovacancies, instead of vacancies.

The strategy of comparing dynamics with the one of a faster unconstrained model and reconstructing the moves of the latter by a proper path of allowed moves can be also used to derive upper bounds for the density and size dependence of the relaxation time, τ, for non-cooperative KCLG and KCSM (see [40] and [23], respectively). The paths are always constructed using the fact that, if there is a macrovancancy (defect), we can move it everywhere and facilitate any nearest neighbor jump (birth/death) of particles. Therefore comparison with the unconstrained model in general gives an extra

factor $(1-\rho)^q$ (the cost of creating the mobile region) times a term related to the length of the path (which can bring a dependence both on the lattice size, L, and on ρ). Note that in principle also an entropy term should be accounted (for the bounds on τ and D_s), counting all the possible configurations which have to pass trough the same bottleneck [23, 36, 40]. However, this is just a constant factor for non cooperative models (more precisely it is the entropy on a number of sites proportional to the size of the macrovacancy) and cannot change the scaling in $1-\rho$.

From results in [23, 40], one has that for non-cooperative models the dependence of τ on the lattice size L is the same as for models without constraints: $\tau \propto L^2$ for KCLG, τ bounded by a finite constant uniformly in L for KCSM (where τ is the inverse of the spectral gap of the Lioviullian operator, see [42]). On the other hand, since relaxation occurs trough the macrovacancies which become rarer at higher density, the density dependence is different. For example, for KA on a triangular lattice with particle sources at the boundary, we find $L^2/(1-\rho)c_l < \tau < L^2/(1-\rho)^2 c_u$, to be compared with $c_l\, L^2 < \tau < c_u\, L^2$ for SSEP.

5 Jamming percolation on Bethe lattices

Bethe lattices (or in the mathematical literature random c-regular graphs) are often used in the physics literature as an approximation of finite dimensional, e.g. hyper-cubic, lattices. Because locally they have a Cayley tree structure with connectivity $k+1$, their analysis is greatly simplified and one can often obtain exact results on the thermodynamics and the dynamics of the model embedded on them. For proper choices of the constraints, KCMs display a jamming transition on Bethe lattice [35, 51] and, thus, provide an almost solvable example of jamming transition. In the following we present a summary of the results that have been obtained focusing on a simple case: the f-facilitated Fredrickson-Andersen model on a Bethe lattice with connectivity k (we consider $k \geq f > 1$ in order to avoid any finite blocked cluster). The results remain qualitatively the same for particle models but they are more tedious to derive [36].

As discussed previously, a jamming (and ergodic) transition for FA models will take place if and only if at a certain density an infinite cluster of blocked (jammed) particles appears. All the particles inside this cluster must have at least f blocked neighbors in order to be blocked themselves. Thus, this
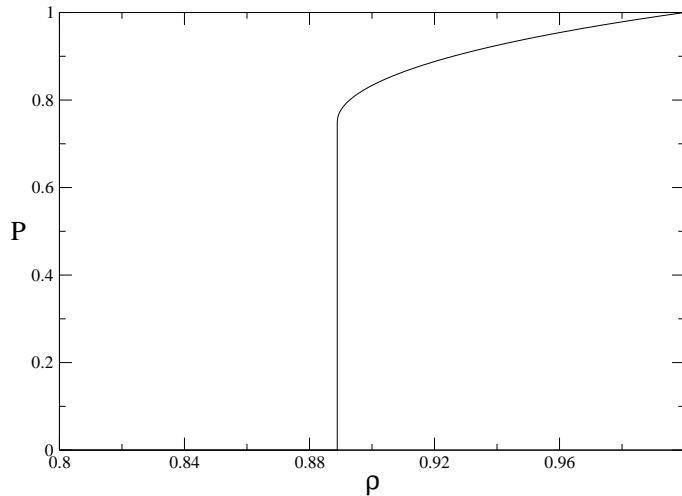
Figure 4: Solution of the equation (2) as a function of ρ for $k = 3$ and $f = 2$.

infinite cluster is the spanning cluster of the so called $f-$core percolation [45], (or bootstrap percolation [52]) a problem that has received a lot of attention recently [53–55].

For a given site the Bethe lattice local structure is Cayley-tree like with k branches going up from each node and one going down. Using this crucial feature it is easy to write a self-consistent equation on the probability P that a site is occupied by a blocked particle (belongs to the $f-$core) because it has more than $k - f + 1$ neighboring particles above it which are blocked (without taking advantage of vacancies below) [52]:

$$P = \rho \sum_{i=0}^{f-1} \binom{k}{i} P^{k-i}(1 - P)^i. \tag{2}$$

Except for $k = f$ for which the transition is continuous, the solution of this equation leads to $P = 0$ for $\rho < \rho_c$ and $P = P_c + O(\sqrt{\rho - \rho_c})$ with $P_c > 0$, see the example for $k = 3$ and $f = 2$ in Fig. 4. The number of blocked particles or the number of sites belonging to the $f-$core are polynomial functions of P that can be derived easily and that have the same behavior of P. They are at the same time discontinuous as in first order phase transitions and singular because of the square root, as in second order phase transitions.

The mechanism behind this behavior has been understood in detail [53,

19

54]. In particular the singular square root behavior is due to the extreme fragility of the infinite spanning jammed cluster at the transition and to the existence of a related diverging lengthscale. In fact, close to the transition, a given jammed particle is connected to clusters of jammed particles that are only marginally blocked, i.e. such that removing only one of their blocked neighbors is enough to unblock them. These clusters form the so called *corona* of the infinite jammed cluster (or $f-$core spanning cluster). The size distribution of corona clusters can be computed analytically [53] and it has been found that their average size diverges at the jamming ($f-$core percolation) transition as $1/\sqrt{\rho - \rho_c}$ coming from the jammed phase. This explains the singular square root behavior found previously [53]: roughly speaking, decreasing the temperature from $\rho_c + \epsilon$ to, say, $\rho_c + \epsilon/2$ (where $0 < \epsilon << 1$) one unblocks first a number of particles proportional to $N\epsilon$. However, unblocking a particle unblocks also all the marginally blocked (corona) particles attached to it. This leads to a "domino effect" such that the effective number of unblocked particles is $N\epsilon \times 1/\sqrt{\epsilon}$, i.e. the net change in the fraction of blocked site is $\sqrt{\rho - \rho_c}$. Since corona clusters, i.e. marginally stable clusters, percolate at the transition one expects an associated diverging lengthscale. This is indeed the case, see [53, 54]: coming from the jammed phase there is lengthscale that diverges as $(\rho - \rho_c)^{-1/4}$.

The analysis of the jamming transition coming from the unjammed phase is much more difficult and one has to resort to numerical simulations. In [34, 51] the persistence,

$$P(t) = \frac{1}{N} \sum_i \langle \Omega_i(t) \rangle$$

where $\Omega_i(t)$ equals one if the site i has remained in the same state (empty or occupied) from time 0 to time t and zero otherwise, and the occupation variable correlation function,

$$C(t) = \frac{1}{N} \sum_i \langle \eta_i(t)\eta_i(0) \rangle$$

have been measured starting from equilibrium initial conditions. We plot in Fig. 5 the persistence as a function of time for the $f = 2, k = 3$ case. Different curves corresponds to different densities approaching the critical point [3]. The

---

[3]Note that in the work [51] we used a different terminology: spin instead of occupation variables and temperature instead of density. The relationship between density and temperature T is $\rho = 1/(1 + e^{-1/T})$.
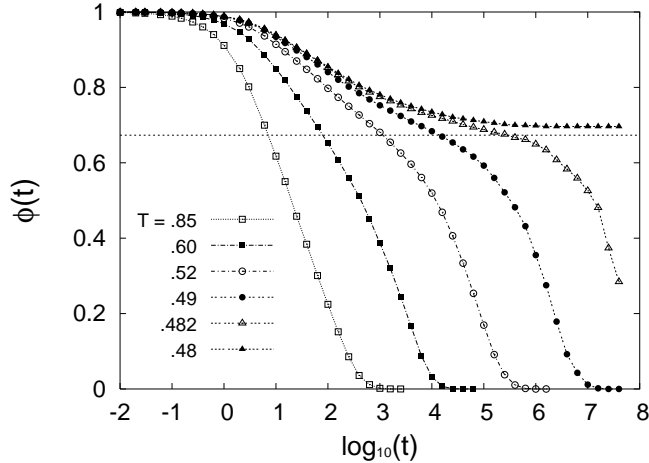
Figure 5: Persistence as a function of time for the $f = 2$, $k = 3$ case for different temperatures approaching the critical temperature $T_c \simeq 0.48$.

correlation has a similar behavior [34]. The existence of the plateau is a direct consequence of the discontinuous character of the jamming transition: the fraction of blocked particles is strictly positive at the transition coming from the jammed phase instead it is zero coming from the unjammed one. This translates into a dynamical behavior such that $\lim_{\rho \nearrow \rho_c} \lim_{t \to \infty} P(t) = 0$ and $\lim_{t \to \infty} \lim_{\rho \nearrow \rho_c} P(t) > 0$ and equal to the fraction of blocked sites. Associated to the non-commutation of these two limits there is a diverging time scale, the time on which $P(t), C(t)$ equals, say, half of their plateau value. The numerics indicates that it follows a power law divergence $\tau \propto (\rho_c - \rho)^{-\gamma}$ with $\gamma \simeq 2.9$.

Finally, it has been found a diverging dynamical lengthscale associated with the divergence of the timescale [51] (let us recall that no static correlation can be found because the equilibrium measure is uncorrelated from site to site). In order to unveil this length one has to focus on the fluctuations of the persistence or the correlation [57]. These are encoded in the dynamical susceptibility

$$\chi(t) = N \langle \left[\frac{1}{N} \sum_i \Omega_i(t) - \frac{1}{N} \sum_i \langle \Omega_i(t) \rangle \right]^2 \rangle / T$$

$\chi(t)$ develops a peak (see Fig.6) for $t \propto \tau$ that diverges for $T \nearrow T_c$. This

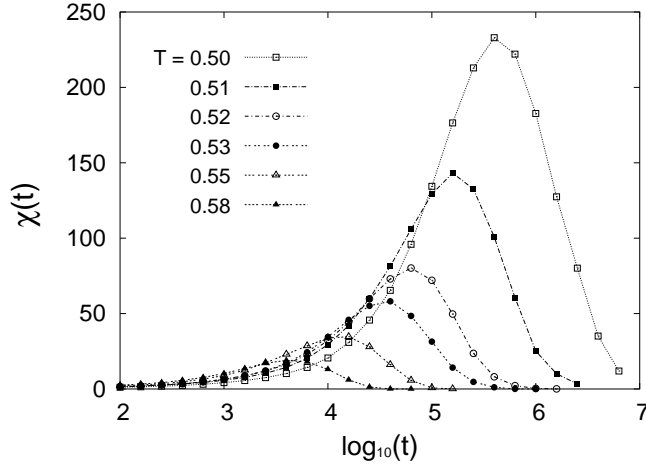Figure 6: Equilibrium dynamical susceptibility $\chi(t)$ vs time t at temperature T. System size $N = 2^{14}$.

divergence is related to the fact that close to T_c more and more particles have to evolve in a correlated way in order to make the system relax. Note that, exactly as for ferromagnets the divergence of the fluctuations of the magnetization is a signature of a diverging lengthscale, so it is the divergence of the peak of $\chi(t)$ at the jamming transition. However, the precise characterization of this dynamic lengthscale and its relationship with the results on the jammed phase have still to be worked out.

Let us summarize the features of the jamming transition found on the Bethe lattice. It has a *first order* character because the fraction of jammed particles and the long-time limit of correlation and persistence functions (called in spin-glasses the Edwards-Anderson parameter) are discontinuous at the transition. At the same time it is characterized, as *second order* phase transitions, by a diverging timescale and diverging lengthscales. Although the detailed connection between time and lengthscales (from the jammed and unjammed phase) has still to be worked out from numerics it seems clear that all these quantities diverge as power law in $|\rho - \rho_c|$. It is interesting to note that qualitatively these features are also shared by mean-field disordered systems, as p-spins models, close to their dynamical transition and the Mode Coupling Theory of the glass transition [6]. The following section is devoted to the analysis of jamming transitions in finite dimensional models. As we

will see some of the features found on the Bethe lattice persist, for example the mixed (first and second order) character of the transition. Instead others, as the divergence of the relaxation times, change and actually become closer to what expected for glass-jamming transitions: now the logarithm of τ diverges as a power law in $|\rho - \rho_c|$, i.e. in a Vogel-Fulcher like form.

6 Jamming percolation on finite dimensional lattices

In this Section we give an extended explanation of the results obtained in collaboration with D.S.Fisher [15,37] for the Knight models defined in Section 2. As already mentioned an *ergodicity breaking transition* occurs at $\rho_c < 1$: above ρ_c a finite fraction of the system is frozen. This is due to an underlying percolation transition for the clusters of mutually blocked particles, which we called *jamming percolation*.

Let us give a brief summary of the main results letting for the next sections their derivation.

As discussed in Section 3 the dynamical transition of the Knight models can be studied using the following cellular automata [37]. Start from an initial configuration sampled with equilibrium measure, μ_ρ, then empty an occupied site if the constraint is satisfied. Then continue the procedure until no more particles can be removed. This final configuration is either completely empty or one that contains a percolating cluster of particles which do not satisfy the constraint. Let us call ρ_∞ the density of this final configuration. We will show that at the critical density of site directed percolation on a square lattice, $\rho_{dp} \simeq 0.705$, a discontinuous percolation transition occurs: $\rho_\infty = 0$ for $\rho < \rho_{dp}$ and $\rho_\infty > 0$ for $\rho \geq \rho_{dp}$. Since the final backbone for this cellular automata contains all the particles that are frozen under the stochastic evolution of Knights, we conclude that below ρ_{dp} Knight model is ergodic and ergodicity is broken above. Furthermore, the fraction of the system which is frozen coincides with ρ_∞ and has a finite jump at the transition.

As for the FA on a Bethe lattice, we find that the dynamical transition transition has a *first order* character with a discontinuous Edwards-Anderson parameter and, at the same time, is characterized by diverging time and lengthscales, as second order like transitions.

The diverging lengthscale can be determined studying finite size effects. Consider the model on a finite lattice Λ_L with periodic boundary conditions and evaluate the probability $R(L, \rho)$ that it can be completely emptied by allowed moves, i.e. the probability that Λ_L is *internally spanned*. Since at any fixed density $\rho < \rho_{dp}$ the final backbone of the cellular automata is empty, $R(L, \rho)$ goes to one in the thermodynamic limit. On the other hand, if the limit $\rho \nearrow \rho_{dp}$ is taken first, $R(L, \rho)$ goes to zero. The relevant length $\Xi(\rho)$ is the crossover length which separates the two regimes: $\lim_{L\to\infty, \rho \nearrow \rho_{dp}} R(L, \rho) = 0$ for $L/\Xi(\rho) \to 0$ and $\lim_{L\to\infty, \rho \nearrow \rho_{dp}} R(L, \rho) = 1$ for $L/\Xi(\rho) \to \infty$. In other words, $\Xi(\rho)$ is the dynamical length which corresponds to the typical size of blocked clusters (i.e. the incipient percolating clusters for jamming percolation). As we will explain, by analytical arguments we find [15] that $\log \Xi(\rho) \simeq (\rho - \rho_{dp})^{-\mu}$. Here $\mu = \nu_\parallel (1 - z)$ where $\nu_\parallel \simeq 1.73$ is the critical exponent of the parallel directed percolation (DP) correlation length, $\xi_\parallel \simeq (\rho - \rho_{dp})^{-\nu_\parallel}$, and $z \simeq 0.63$ is the exponent relating parallel and transverse DP correlation lengths, $\xi_\perp \simeq \xi_\parallel^z$. We also rigorously proved [4] the upper and lower bounds $c_1 \exp(c_2 \xi_\parallel^{1-z}) < \Xi(\rho) < c_3 \exp(c_4 \xi_\parallel^2)$ [37]. These establish that Ξ diverges faster than power law and the lower bound coincides with the value we expect for Ξ.

Due to this diverging length, the relaxation time τ should diverge as Ξ^z with $z \geq 2$. Indeed, relaxation should require the diffusion of regions of density Ξ (see [36] for similar results for FA model). In [23] the rigorous bound $\tau \geq \Xi$ is proved, where τ is the inverse of the spectral gap of the Lioviullian operator $\mathcal{L}$ (i.e. the worst relaxation time on all one time quantities). Therefore Knight models exhibit a Vogel-Fulcher like relaxation: the log of times diverge as power law when the critical density is approached. This is different from the findings for FA model on Bethe lattices, were τ diverges as power law (see Section 5). Since in the Knights model there are no static interactions between the particles it is clear that their glass-jamming transition is purely dynamical and not related to any thermodynamic transition.

In the following we shall explain the arguments leading to the proof of an ergodicity breaking transition at ρ_{dp} and of its mixed first/second order char-

---

[4] The existence of the two different correlation lengths, which are due to the asymmetry of DP and the power law divergence of $\xi_\parallel$, are given for granted in physical literature. Indeed, they have been verified both by numerical simulations and analytical works trough renormalization technique (see [56] for a review). However, a rigorous mathematical proof of these results for DP is still lacking. Our bounds for Ξ are rigorous modulo the assumption $\xi_\perp = \xi_\parallel^z$, $z < 1$.
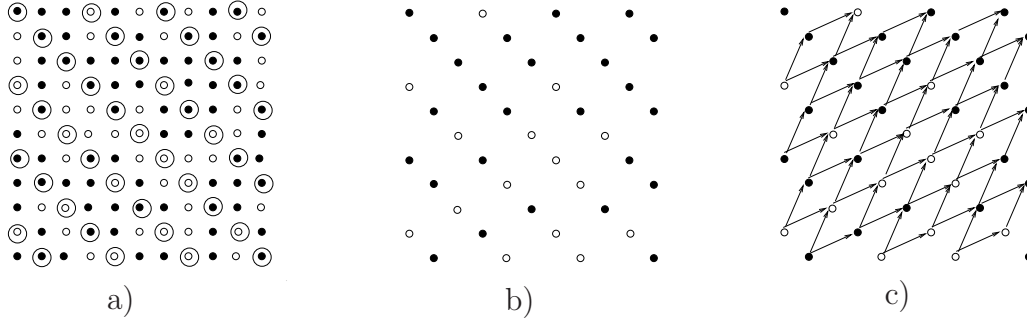
Figure 7: a) Sites inside circles are those obtained starting form the origin and choosing its NE and SW neighbours and the NE and SW neighbours of the latter and so on. b) Sublattice obtained erasing all sites from the square lattice except those inside circles c) Oriented sublattice: arrows go from each site to its two NE neighbours (w.r.t. the original lattice)

acter (we refer to [37] for rigorous proofs). These will unveil the mechanism which induces these remarkable properties which are typical of an ideal glass transition. Also, it will be clear why we choose the specific form of Knight constraints and how one can modify or generalize them to higher dimension keeping a transition with the same character.

6.1 Ergodicity breaking for $\rho > \rho_{dp}$

Let us prove that ergodicity is broken above ρ_{dp}, namely a finite fraction of sites is frozen. This is equivalent to showing that the origin belongs with finite probability to a percolating cluster of frozen sites. Here, as in [15], we call a site *frozen* if it cannot be unblocked even by first emptying with allowed moves an arbitrarily large number of sites. Consider the sublattice which is obtained from the square lattice by erasing all sites except the origin, its North-East and South-West neighbors, the North-East and South-West neighbors of the latter and so on as in Fig. 7 a), b). Then construct a directed graph on this sublattice by drawing arrows connecting each site to its North-East neighbors as in Fig. 7 c). Notice that this corresponds simply to a two dimensional square lattice (only rotated and squeezed). Also, since there are no static correlations in the equilibrium measure, if the configuration on the original lattice is chosen with μ_ρ, the same holds for the configuration on the sublattice. Therefore the results for site Directed Percolation [56] imply that,

if $\rho > \rho_{dp}$, the origin belongs with finite probability to an infinite directed (i.e. following the direction of the arrows) percolating cluster of occupied sites. It is now easy to check that if we restore the whole lattice and consider Knight dynamics, all sites belonging to the cluster which percolates on the sublattice are frozen: *a finite fraction of the system is frozen above* ρ_{dp}. Indeed, each of these sites has at least one occupied NE neighbor and at least one occupied SW neighbour, therefore it is blocked along NE-SW diagonal. In the following, we call *NE-SW cluster* a directed occupied path on the sublattice obtained with the procedure above. The definition is analogous for the *NW-SE cluster*, where the sublattice is the one constructed erasing all sites but the origin, its NW and SE neighbours and so on. Note that in order to establish the existence of frozen clusters we have not used the possibility of blocking along the NW-SE diagonal. On the other hand, this should be taken into account if we want to show that a given configuration does not contain frozen sites as we will do in the following section.

6.2   Ergodicity for $\rho < \rho_{dp}$

Let us prove that the system is ergodic in the thermodynamic limit for $\rho < \rho_{dp}$, which corresponds to showing that the fraction of frozen sites is zero. Note that if the rule contained blocking only along one of the two diagonals, ergodicity would follow immediately from the fact that occupied directed paths do no percolate below ρ_{dp}. However, for the constraints we have chosen, a percolating directed path implies a frozen cluster but the converse is not true. Indeed, due to the fact that a site can be blocked along either the NE-SW or the NW-SE diagonal or both, a NE-SW cluster can be blocked either if it spans the lattice or if it is finite but both its ends are blocked by a T-junction with NW-SE percolating paths (see Fig. 8 a)). By using such T-junctions it is also possible to construct frozen clusters which do not contain neither a spanning NE-SW nor a spanning NW-SE cluster: all NE-SW (and NW-SE) clusters are finite and are blocked at both ends by T junctions by finite NW-SE (NE-SW) ones (see figure 8 b)). As we will show in detail, these T-junctions are crucial to make the behavior of jamming percolation very different from site directed percolation although the two transitions share the same critical density.

Let us now show how the proof or ergodicity below ρ_{dp} works. The strategy consists in constructing a set of configurations, $\mathcal{F}_L$, on Λ_L and show that $\mathcal{F}_L$ are internally spanned and $\lim_{L\to\infty} \mu_\rho(\mathcal{F}_L) = 1$. This, as explained in

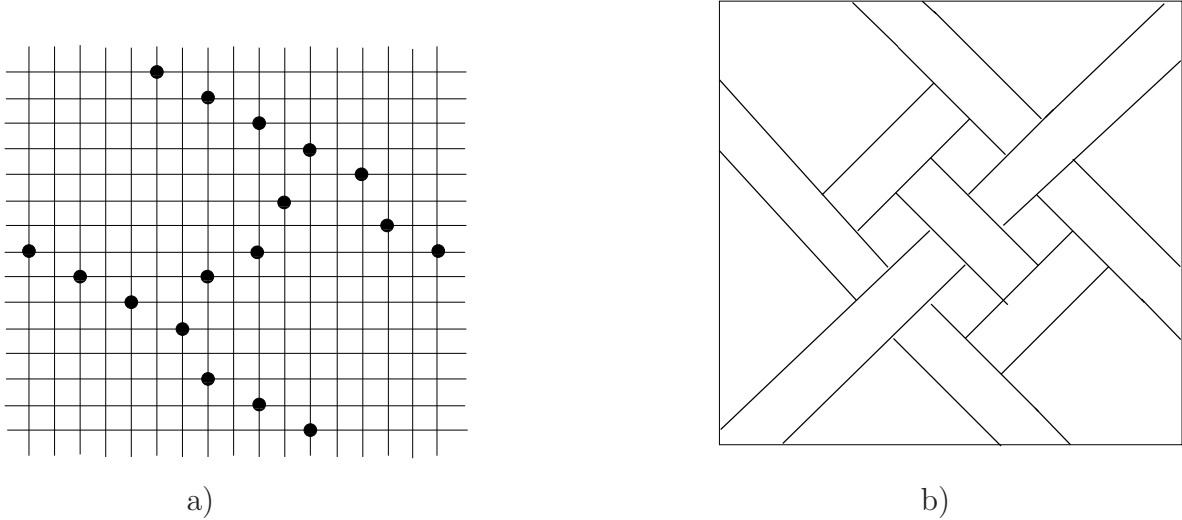a)   b)

Figure 8: a) A NE-SW non spanning cluster blocked by T-junctions with two NW-SE spanning clusters; b) Segments parallel to the NE-SW (NW-SE) diagonal stand for NE-SW (NW-SE) clusters. The depicted structure is blocked, even if it does not contain neither a NE-SW nor a NW-SE spanning cluster

Section 3, concludes the proof of ergodicity for $\rho < \rho_{dp}$ and (together with results in previous section) establish that ergodicity breaking occurs at ρ_{dp}.

Consider a configuration within which there is an empty square of size $n \times n$ and focus on the sufficient conditions to empty the next shell, i.e. to construct an allowed path which empties the $n+2 \times n+2$ square. The initial vacancies guarantee that we can empty a centered segment of length $n-4$ external to each side. Consider for example site x in fig. 9 a), both its SW and SE couples are inside the empty square: the constraint is satisfied on both diagonals and x can be emptied. It is immediate to check that, even if the rest of the lattice is occupied, this procedure can be continued until emptying the triangular structure above each side depicted in Fig. 9 b). This is formed by centered lines whose length decreases of four sites at each step, therefore its overall height is $I(n/4)$ where $I(x)$ stands for the integer part of x. In order to empty the $n + 2 \times n + 2$ square, five sites remain to be emptied on each corner: those indicated by question marks in Fig.9 b). Consider for example one of these site on the top left corner, indicated as y in Fig.10. The constraint along the NW-SE diagonal is verified, since both
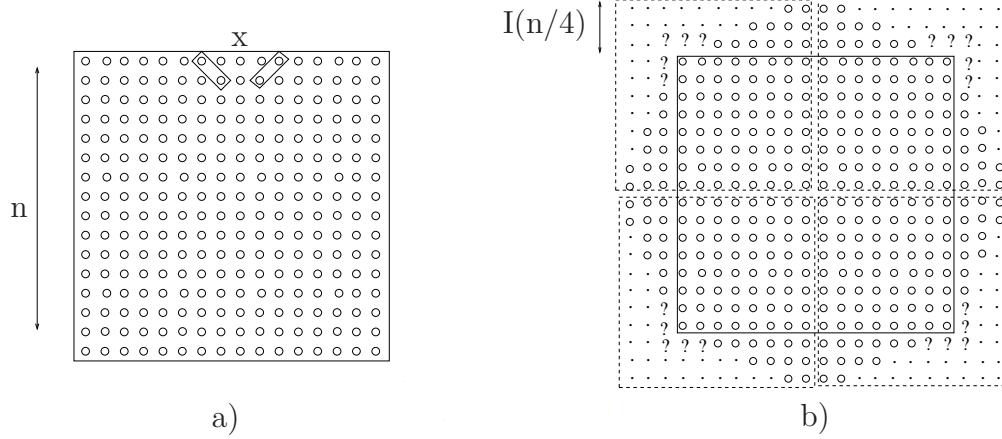
27

Figure 9: a) The empty $n \times n$ square. Site x can be emptied since its SE and SW neighbours are all inside the empty square. b) The triangular structure of height $I(n/4)$ which can be emptied above each side. ? denotes the 5 sites on each corner which are not guaranteed to be emptied (unless a proper condition is fulfilled by the configuration outside the empty $n \times n$ nucleus).

its SE neighbors are inside the empty square. Instead, since neither the NE nor the SW couples are contained in the empty region, y can be blocked along NE-SW diagonal and in this case we cannot empty it. However, it is possible to derive a necessary condition for y to be frozen, which gives in turn a sufficient condition to construct an allowed (i.e. verifying the constraint at each elementary move) path in the configuration space which allows to empty y. Focus on the square of size $n/2 + I(n/4)$ centered on the top left corner and containing half of the triangular structure associated to the up and left sides, i.e. the square inside the dashed region in Fig. 9b). Consider the sublattice constructed from y inside this square by erasing all sites except its North-East and South-West neighbors and so on (as we did for the origin in figure 7). It can be directly checked that y can be frozen only if it belongs to a NE-SW path, i.e. a directed path on this sublattice, which spans the square (see Fig. 10). This is due to the fact that any occupied cluster along the NW-SE diagonal can be unfrozen if it terminates inside the empty region ($n \times n$ square plus triangular region). Therefore, a sufficient condition to construct an allowed path to empty y (and the other remaining four sites at the top left corner) is that in the dashed square region there is not a percolating NE-SW
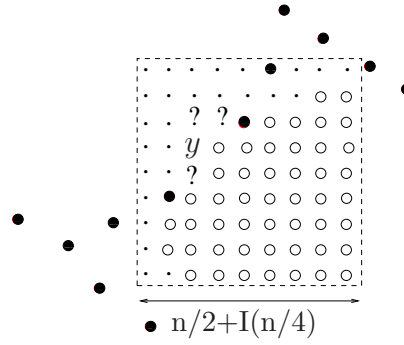
28

Figure 10: Here we depict the top left square in Fig. 9 b) and show the necessary condition for y to be frozen: it should belong to a NE-SW cluster spanning the dashed square. Otherwise: if one of its end is free it can be unblocked from there; if they are both blocked by T-junctions with NW-SE clusters these terminate inside the empty region and can be unblocked from there.

cluster. Since the size of this region is proportional to n and $\rho < \rho_{dp}$, such a cluster occurs with a very small probability, $\exp(-n/\xi_\parallel)$ for large n with $\xi_\parallel$ the parallel correlation length for DP [56]. As a consequence the probability of emptying y increases at least exponentially fast to one when the size of the empty nucleus, n, is increased. The same argument can be applied to the other four sites indicated by question marks and to those on the other three corners of the lattice, concluding that the probability $P(n \to n+2)$ to go from the empty $n \times n$ to the empty $n + 2 \times n + 2$ nucleus is bounded from below by $(1 - 20\exp(-n/\xi_\parallel))$. Thanks to the exponential increase towards one, the probability that this procedure can be continued up to infinite size stays strictly positive because it is bounded from below by $\prod_{i=n}^{\infty} P(i \to i+2) > 0$. Finally, using the $O(L^2)$ different positions for the initial empty nucleus, we conclude that the probability for Λ_L to be internally spanned converges to one in the thermodynamic limit at any $\rho < \rho_{dp}$. This is due to the fact that, in order to prevent the expansion of a large empty nucleus, we should require long DP clusters, which are highly improbable below ρ_{dp}.

6.3 Discontinuity of the transition

Results in Sections 6.1 and 6.2 prove that an ergodicity breaking transition occurs for Knights at ρ_{dp}, due to the percolation transition of blocked structures. In the present and the following section we show that this transition, which we call *jamming percolation*, have features which are qualitatively different from those of DP and any conventional percolation transition. Indeed it is discontinuous, i.e. the density of the frozen clusters have a finite jump at the transition (the critical clusters are compact rather than fractal) and their typical size increases faster than any power law when $\rho \nearrow \rho_{dp}$.

In order to prove discontinuity we construct a set of configurations which have finite probability on the infinite lattice at ρ_{dp} and show that the origin is frozen for all these configurations. We will make use of the blocked structures containing T-junctions among NE-SW and NW-SE clusters which have been introduced in Section 6.2. Consider a configuration in which the origin belongs to a NE-SW path of length $\ell_0/2$: this occurs with probability p_0. Now focus on the infinite sequence of pairs of rectangles of increasing size $\ell_i \times \ell_i/12$ with $\ell_1 = \ell_0$, $\ell_i = 2\ell_{i-2}$ and intersecting as in Fig.11. If *each* of these rectangles with long side along the NE-SW (NW-SE) diagonal contains a NE-SW (NW-SE) percolating path (dotted lines in Fig. 11 b)), the origin is frozen. This can be directly checked: an infinite backbone of
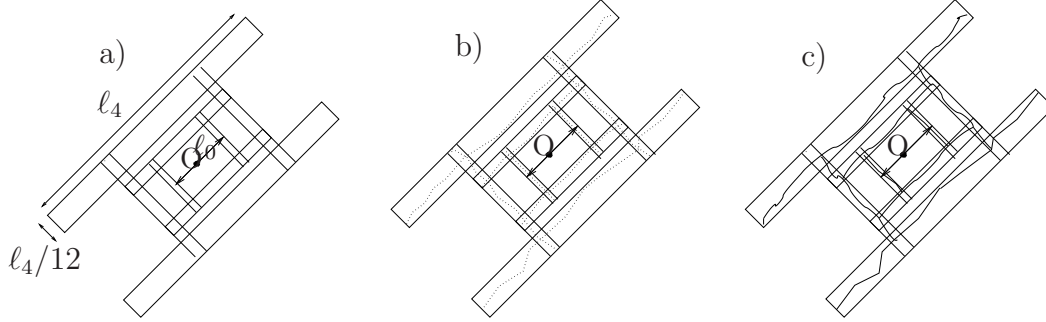
Figure 11: a) The sequence of intersecting rectangles of increasing size $\ell_i \times 1/12\ell_i$ describer in the text. b) Dotted non straight line stand for NE-SW (NW-SE) clusters spanning the rectangles with long side in te NE-SW (NW-SE) direction. c) Frozen structure containing the origin

mutually blocked particles constituted by pieces of these paths connected by T-junctions (continuous line in Fig. 11 c)) occurs. Therefore the probability that the origin is frozen, $q(\rho)$, is bounded from below by

$$q(\rho) > p_o \prod_{i=1,\infty} P(\ell_i)^2$$

where $P(\ell_i)$ is the probability that a rectangle of size $\ell_i \times 1/12\ell_i$ with short side in the transverse direction is spanned by a DP cluster. This probability converges to one exponentially fast in ℓ_i due to the anisotropy of critical clusters for directed percolation. Recall that there are a parallel and a transverse length for DP with different exponents, i.e. a cluster of parallel length ℓ has typically transverse length ℓ^z. Let us divide the $\ell_i \times 1/12\ell_i$ rectangle into ℓ_i^{1-z} slices of size $\ell_i \times 1/12\ell_i^z$. For each slice the probability of having a DP cluster along the parallel direction at ρ_{dp} is order unity. Thus, the probability of *not* having a DP cluster in each of the slice is $1 - P(\ell_i) = O[\exp(-c\ell_i^{1-z})]$. From this result and above inequality for q, it follows immediately $q(\rho_{dp}) > 0$.

Therefore the infinite cluster of jamming percolation is "compact", i.e. of dimension d at the transition. Note that to obtain discontinuity two ingredients of the constraints were crucial: the existence of two transverse blocking directions each with an underlying percolation transition; the anisotropy of these transitions. Indeed, anisotropy is necessary to have the increase towards one of the probability that above rectangles are spanned when their size is increased. In turn, this is necessary to get a finite probability for the

construction which freezes the origin.

6.4 Dynamical correlation length

In this Section we explain the arguments in [15] leading to the result $\log \Xi(\rho) \simeq k(\rho - \rho_{dp})^{-\mu}$ for $\rho < \rho_{dp}$, where $\mu = \nu_{\parallel}(1 - z) \simeq 0.64$. As already explained, $\Xi(\rho)$ is the crossover length dividing the regime in which the probability for a finite region to be internally spanned goes to zero or to one when $\rho \nearrow \rho_{dp}$, i.e. the length below which finite size effects are important. For jamming percolation it corresponds to the diverging size of the incipient spanning clusters and for Knight models to the typical size of the region that has to be rearranged to unblock a given site. Let us sketch separately the arguments leading to $\log \Xi(\rho) \geq k_l(\rho - \rho_{dp})^{-\mu}$ and to $\log \Xi(\rho) \leq k_u(\rho - \rho_{dp})^{-\mu}$ with k_l, k_u two positive constants.

To establish the lower bound we construct a set of configurations containing a frozen backbone and we show that the probability of this set goes to one when $\rho \nearrow \rho_{dp}$ and $L \to \infty$ with $\log L \leq k_l(\rho - \rho_{dp})^{-\mu}$. Again, we make use of the T-junctions described in Section 6.2. Consider the set of NE-SW and NW-SE paths of length s intersecting as in Fig. 12.

As can be directly checked, this structure can be emptied only starting from its border since each finite directed path terminates on T-junctions with paths in the opposite direction. Therefore, if the construction is continued up to the border and we consider periodic boundary conditions, all sites in the structure are frozen. Furthermore, a similar frozen backbone exists also if one or more of these paths is displaced inside an adjacent rectangular region of size $s \times s/6$, as shown in Fig. 12. Therefore the probability that the regions is not internally spanned, $1 - R(L, \rho)$, is bounded from below by the probability that *each* of these rectangles contains at least one path connecting its short sides. This leads to

$$R(L, \rho) \leq n(L, s) \exp(-cs^{1-z}) \tag{3}$$

where $n(L, s) = O(L/s)^2$ is the number of the rectangles contained in the structure and $\exp(-cs^{1-z})$ is the probability of not having a DP path in a region $s \times s/6$ as long as $s \leq \xi_{\parallel}$ (see previous section). The inequality (3) leads to $\lim_{L \to \infty, \rho \nearrow \rho_{dp}} R(L, \rho) = 0$ for $\xi_{\parallel} \exp(c\xi_{\parallel}^{1-z})/L \to \infty$, therefore $\log \Xi \geq k_l(\rho - \rho_{dp})^{-\mu}$.

On the other hand, in order to establish the upper bound, we show that for $\log L \geq k_u(\rho - \rho_{dp})^{-\mu}$ there is typically an nucleus of vacancies which
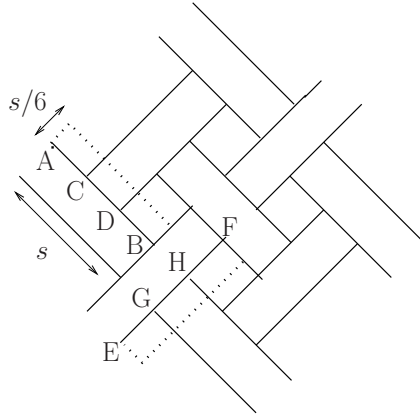
Figure 12: The frozen structure described in the text: continuous lines stand for occupied NE-SW or SW-NE clusters (for simplicity we draw them as straight lines, recall however that they will in general bend since they have two bending directions). Each of these clusters is blocked since it ends in a T-junction with a cluster along the transverse diagonal. The dotted rectangle adjacent to cluster AB (EF) are the regions in which this cluster can be displaced and yet a frozen backbone is preserved. Indeed the T-junctions in C and D (G and H) will be displaced but none of them will be disrupted.

can be expanded until emptying the whole lattice. From the results in Section 6.2 it is easy to see that the probability to expand an empty nucleus to infinity is dominated by the probability of expanding it up to $n = \xi_\parallel$. Indeed, above this size the probability of an event which prevents expansion is exponentially suppressed. Therefore, considering the $O(L/\xi_\parallel)^2$ possible position for a regions that it is guaranteed to be emptyable up to size $\xi_\parallel$, we get that the probability that Λ_L is internally spanned is roughly bounded as $R(L, \rho) \geq L^2 \delta$ for $L^2 \leq \delta$, where δ is the probability that a small empty nucleus can be expanded until size $\xi_\parallel$. In the emptying procedure described in Section 6.2 we subsequently increase from n to $n+2$ the size of the empty nucleus. If we require instead that on a region of size $O(\xi_\parallel)$ around each corner there is not a spanning DP cluster, we can expand directly to $\xi_\parallel$. The probability of the latter event gives $\delta \geq \exp(-c\xi_\parallel^{1-z})$ (see [15]). Therefore, we get the desired upper bound on $\log \Xi$ that has the same scaling as the lower bound.

6.5   Numerical Results

In the following we present numerical results on the percolation of blocked structures that support our theoretical findings. Starting from an initial configuration we sequentially pick away all particles that are not blocked, so that the final configuration contains the backbones of forever blocked particles. In Fig. 13 we show the probability that a site belongs to the infinite spanning cluster for lattice sizes $N = 100^2, 200^2, 400^2, 800^2, 1600^2$ averaged over 40000 samples. Though the transition takes place at the critical density of DP $\rho_{dp} \simeq 0.701$, as we have proved, finite size effects appear already at $0.53 - 0.55$.

Indeed, the probability that there *exists* a frozen cluster is substantial for ρ fifteen percent below ρ_c even in our largest systems, $(L = 1600)$: it is thus hard to study the asymptotic critical behavior (see [58] for an analogous problem in the context of bootstrap percolation). But in a slightly different model one can get closer to the transition [33]: these data are consistent with the predicted $\ln \Xi \sim (\rho_c - \rho)^{-\mu}$ with $\mu \cong 0.64$, but the small range of $\ln L$ available makes the uncertainties in μ large.

Another theoretical finding confirmed by numerics is the first order character of the transition. Indeed the histograms of the density of blocked structures, ρ_b, clearly show a well defined two peak shape as in usual first order transitions (see inset of Fig. 13). The peak at a non zero density is
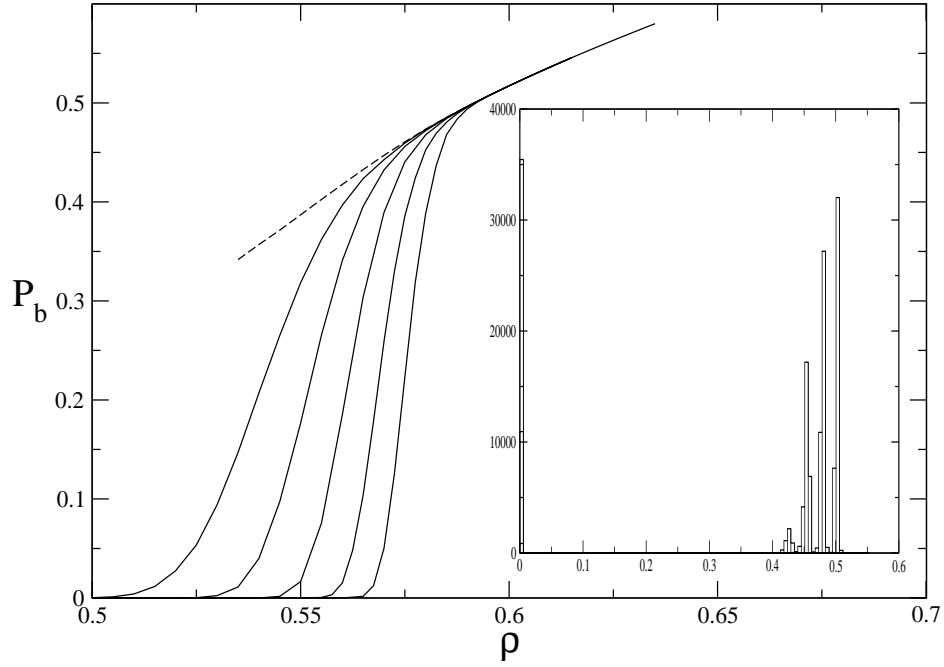
Figure 13: Probability that a site belongs to the infinite blocked spanning cluster as a function of the initial density for system sizes $N = 100^2, 200^2, 400^2, 800^2, 1600^2$ averaged over 40000 initial configurations (from left to right respectively). Inset: histograms of the number of initial configurations (y axis) leading to a fraction of sites ρ_b (x-axis) for $N = 800^2$, 40000 initial configurations and initial density $\rho = 0.5775, 0.5825, 0.5875, 0.5925$ (when increasing the initial density the right peak moves to the right).
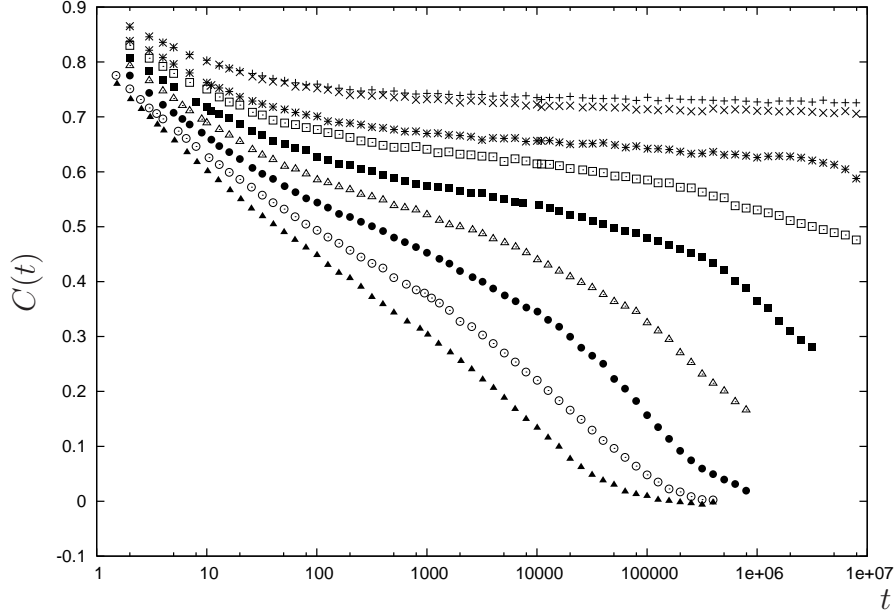
Figure 14: Density density correlation as a function of time (MonteCarlo steps) for a 100×100 lattice. From bottom to top, $\rho = 0.49, 0.50, 0.51, 0.52, 0.53, 0.54, 0.55, 0.56, 0.57$.

clearly distinct from the one at zero density and moves to the right by increasing the density of particles in the initial configuration, thus showing that asymptotically the transition is first order. Furthermore there are no finite size effects on the peak position but only on its weight. Thus, the continuous curves $P_b(\rho)$ in Fig. 13 are the average of two curves: the trivial one, $P_b = 0$, corresponding to the left peak and the dotted one corresponding to the right peak. By changing the system size the weights of the two peaks change and so the continuous averaged $P_b(\rho)$ shifts to the right.

Finally, let's focus on the predictions for the dynamics. First, as already discussed, an ergodicity breaking transition occurs at $\rho = \rho_{dp}$. Furthermore, the first-order character of the percolation of blocked structures implies a discontinuous jump of $q_{EA}(\rho) = \lim_{t \to \infty} < \eta_x(t)\eta_x(0) >_c$. This is the plateau of the correlation function, see Fig.14 and is the analog of the Edwards-Anderson parameter in spin-glasses. In fact for $\rho < \rho_c$, ergodicity implies that $q_{EA}(\rho) = 0$ since the system always relaxes to equilibrium. Instead for $\rho \geq \rho_c$, by separating the contribution from sites which are occupied and

blocked forever and the remaining sites, one can show that $q_{EA}(\rho) \geq c(\rho)q(\rho)$ [15, 37], where $c(\rho)$ is a strictly positive for all $\rho < 1$ and $q(\rho)$, as defined previously, is the probability the the origin is frozen. Therefore, $q_{EA}(\rho) > 0$, for $\rho \geq \rho_{dp}$.

Furthermore the relaxation timescale, τ, diverges also very fast at the transition as discussed previously. As a check, we performed numerical simulations of standard Montecarlo dynamics. The results for $< \eta_x(t)\eta_x(0) >_c$ are plotted in Fig. 14 for system size $N = 100^2$. The curves clearly shows a developing (discontinuous) plateau which becomes infinite after a certain (size dependent) density. However, the initial curves until $\rho = 0.53$ have no finite size effects. This shows that the developing of a discontinuous plateau and the increasing of the timescale start far from the critical density, in agreement with an essential singularity for the laws for Ξ, τ (for a power law divergence τ should diverge much closer to ρ_c). Note that, because of the very severe finite size effects, one needs much larger system sizes (and much larger timescales) in order to measure successfully the exponent of the essential singularity. We leave that for future study.

7 Conclusion

As discussed in this work cooperative KCMs display a remarkable physical behavior. In particular, Knights model undergoes a purely dynamical phase transition due to a jamming percolation : a giant blocked cluster appears at $\rho_c < 1$. This new type of transition has features that are very different from usual (first and second order) phase transitions and that are similar to the ones indeed expected for glass-jamming transitions. In particular the fraction of jammed particles is discontinuous (as for first order phase transition) although time and lengthscales diverge (as for second order phase transitions). Furthermore the relaxation time diverges with a Vogel-Fulcher like form, i.e. much faster than a power law.

The extension and the universality of our results are fundamental open questions. In three dimensions, two natural generalizations of our jamming percolation exist: one composed of DP clusters — which should slow down as a double exponential of $(\rho - \rho_c)^{-\bar{\mu}}$ — and the other of directed sheet-like structures which will have exponential slowing down like we have found in 2D. The key ingredients are kinetic constraints that enable huge jammed clusters to form out of small objects without these becoming much more

common or much larger. A very important issue is whether the mechanism that we devise to create a jamming percolation, which is based on interacting DP clusters, is the only possible one or there are others that may lead to a very similar dynamical transition, see [54].

For the future, the connection between our results and the jamming transition found for continuum particle systems [2] needs exploring. One should analyze the effects of constraint-violating processes occurring with a very low rate: these are certainly present for molecular liquids undergoing a glass transition. Similarly, it would be very important to generalize our results to systems of particles in the continuum. Finally, it would be very interesting to compare the geometrical and statistical properties of jamming percolation clusters to the ones that can be measured in experiments in colloidal and granular systems.

References

[1] P.G.De Benedetti and F.H.Stillinger *Nature* **410**, 267 (2001).

[2] ER.Weeks et al. *Science* **287**, 627 (2000); V.Trappe et al. *Nature* **411**, (2001) 722.

[3] G.Marty, O.Dauchot *Phys.Rev.Lett* **94** 015701 (2005)

[4] M.A.Ediger *Ann.Rev.Phys.Chem.* **51**, 99 (2000); E.Vidal-Russel, N.E.Israeloff *Nature* **408**, 695 (2000); L.A.Deschenes, D.A.Vande Bout *Science* **292** 255 (2001); L.Berthier et al. *Science* **310** 1797 (2005); C.Bennemann et al. *Nature*, **399**, 246 (1999);O.Dauchot, G.Marty, G.Biroli, *Phys.Rev.Lett* **95**, 265701 (2005).

[5] T.R.Kirkpatrick, D.Thirumalai, *Phys.Rev.Lett* **58**, (1987) 2091; T.R.Kirkpatrick, D.Thirumalai, P.G.Wolynes *Phys.Rev.A* **40**, (1989) 1045.

[6] Bouchaud J-P, Cugliandolo L F, Kurchan J and Mézard M, in *Spin-Glasses and Random Fields*, edited by Young A P (World Scientific, 1997).

[7] X. Xia and P.G. Wolynes, PNAS **97** 2990 (2000) and refs therein.

[8] J.-P. Bouchaud and G. Biroli, J. Chem. Phys. **121**, 7347 (2004).

[9] S.Franz *Europhys.Lett.* **73** 492 (2006)

[10] M. Dzero, J. Schmalian, P. G. Wolynes, cond-mat/0502011.

[11] M.A.Moore cond-mat/060241

[12] J. Jackle J. Phys. Cond. Matter **14**, (2002) 1423;

[13] F. Ritort, P. Sollich *Adv. in Phys.* **52** (2003), 219.

[14] G.H.Fredrickson, H.C.Andersen *Phys.Rev.Lett.* **53**, 1244 (1984); *J.Chem.Phys.* **84**, 5822 (1985)

[15] C.Toninelli,G.Biroli, D.S.Fisher*Phys.Rev.Lett* **96**, 035702 (2006).

[16] J.Jackle, S.Eisinger *Z.Phys.B: Cond.Mat.* **84**, 115 (1991)

[17] W. Kob and H.C. Andersen, *Phys.Rev.E* **48** (1993) 4364.

[18] P.Sollich, M.Evans *Phys.Rev.Lett* **83** 3238 (1999)

[19] D.Aldous, P.Diaconis *J.Stat.Phys.* **107** 845 (2002)

[20] J.P.Garrahan, D.Chandler *Phys. Rev.Lett* **89** 035704 (2002)

[21] S.Whitelam, L.Berthier, J.P.Garrahan, *Phys. Rev.Lett* **92**, 185705 (2004); *Phys.Rev.E* **71**, 026128 (2005)

[22] R.Jack, P.Mayer, P.Sollich cond-mat/0601529

[23] N.Cancrini, F.Martinelli, C.Roberto, C.Toninelli cond-mat/0603745

[24] L.Berthier, J.P.Garrahan *J.Chem.Phys.* **119**, 4367 (2003)

[25] J.P. Garrahan, D. Chandler, Proc. Natl. Acad. Sci. **100**, 9710 (2003).

[26] J.Reiter *J.Chem.Phys* **95**, 544 (1991)

[27] G.H.Fredrickson, S.A.Brawer *J.Chem.Phys* **84** 3351 (1986)

[28] M.Einax, M.Schulz *J.Chem.Phys* **115** 2282 (2001)

[29] I.S.Graham, L.Piché, M.Grant, *J.Phys.Cond.Matt*, **5**, 6491 (1993); *Phys.Rev.E*, **55**, 2132 (1997)

[30] P.Harrowell, *Phys.Rev.E* **48**, 4359 (1993)

[31] G.H.Fredrickson *Ann.N.Y.Acad.Sci*, **484**, 185 (1986)

[32] S.Butler, P.Harrowell, *J.Chem.Phys.* **95**, 4466 (1991)

[33] C. Toninelli, G. Biroli and D.S. Fisher in preparation.

[34] L. Berthier, G. Biroli, C. Toninelli in preparation.

[35] J.Reiter, F.Mauch, J.Jackle, *Physica A*, **184**, 493 (1992)

[36] C.Toninelli,G.Biroli, D.S.Fisher *Phys.Rev.Lett.* **92** 185504 (2004); *J.Stat.Phys.* **120**, 167 (2005)

[37] C.Toninelli, G.Biroli cond-mat/0512335

[38] W. Kob, in "Slow relaxations and nonequilibrium dynamics in condensed matter", vol. Session LXXVII of Les Houches Summer School (ed. J.-L. Barrat, M. Feigelman and J. Kurchan), published by EDP Sciences and Springer.

[39] E.R.Weeks, D.A.Weitz *Phys.Rev.Lett.* **89** 095704 (2002); *Chem.Physics* **284**, 361 (2002)

[40] L.Bertini, C.Toninelli *J.Stat.Phys.*, **117**, 549-580 (2004)

[41] C.Toninelli, G.Biroli *J.Stat.Phys.*, **117**, 27-54 (2004)

[42] H.Spohn, *Large scale dynamics of interacting particles* Berlin Springer (1991)

[43] J.Adler *Physica A* **171** (1991) 435

[44] M. Aizenmann, J.L. Lebowitz, *J.Phys.A* **21** (1988) 3801.

[45] Pittel B, Spencer J and Wormald N, *J. Comb. Th. B* **67** (1996) 111.

[46] R.H.Schonmann, *Ann. of Probab.*,**20** (1992), 174-193

[47] C. Kipnis, C. Landim, *Scaling Limits of Interacting Particle Systems*, Grundlheren der Mathematischen Wissenschaften 320, Springer-Verlag, Berlin, New York, 1999.

[48] C.Landim, C.Toninelli in preparation

[49] H.Spohn *J.Stat.Phys.* **59** (19990) 1227; *Physica A* **163**, (1990) 134.

[50] J.Kurchan, L.Peliti, M.Sellitto *Europhysics Lett.* **39** (1997) 365

[51] M. Sellitto, G. Biroli and C. Toninelli. Europhys. Lett. **69** (4), 496 (2005).

[52] Chalupa J, Leath P L and Reich R, *J. Phys. C: Solid State Phys.* **12** (1979) L31.

[53] S. N. Dorogovtsev, A. V. Goltsev, and J. F. F. Mendes Phys. Rev. Lett. **96**, 040601 (2006).

[54] J.M. Schwarz, A.J. Liu, L.Q. Chayes, Europhys. Lett. **73**, 560 (2006).

[55] Abdelaziz Amraoui, Andrea Montanari, Tom Richardson, Rudiger Urbanke, 42nd Allerton Conference on Communication, Control and Computing , cs.IT/0410019. A. Dembo and A. Montanari in preparation.

[56] H.Hinrichsen *Adv. in Phys* **49** 815 (2000)

[57] Franz S and Parisi G, *J. Phys.: Cond. Matter* **12** (2000) 6335

[58] P.De Gregorio, A.Lawlor, P.Bradley, K.A.Dawson Phys.Rev.Lett. **93** (2004) 025501.